Defence Research and Recherche et développement
Development Canada pour la défense Canada

DEFENCE **R&D** DÉFENSE

Computer-aided detection of targets from the CITADEL trial Klein sonar data

John A. Fawcett
Anna Crawford
David Hopkin
Defence R&D Canada – Atlantic

Vincent Myers
NURC, La Spezia, Italy

Benoit Zerr
GESMA, Brest, France

Defence R&D Canada – Atlantic

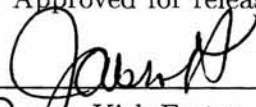Technical Memorandum
DRDC Atlantic TM 2006-115
August 2006

Canada

This page intentionally left blank.

Computer-aided detection of targets from the CITADEL trial Klein sonar data

John A. Fawcett
Anna Crawford
David Hopkin
Defence R&D Canada - Atlantic

Vincent Myers
NURC, La Spezia, Italy

Benoit Zerr
GESMA, Brest, France

Defence R&D Canada – Atlantic

Author

_____

John Fawcett

Approved by

_____

Ron Kuwahara
Head/Signatures

Approved for release by

_____

Kirk Foster
Chair/Document Review Panel

Abstract

In October 2005, DRDC Atlantic participated with NURC (NATO) and GESMA (France) in a joint trial with the remote, semi-submersible vehicle DORADO. A large number of sidescan sonar images of minelike objects on the seabed were obtained for a variety of ranges and aspects. The positions of these dummy targets are very accurately known. In this particular report, we use this data to investigate the performance of 5 simple detection algorithms. Each of the 5 detectors is based upon the outputs of some simple image/filter convolutions. The detections, false alarms, and missed target statistics are presented, as well as an analysis of the missed target statistics as a function of target type and range. The performance of the detectors as their decision threshold is varied (ROC curves) is presented. In addition, the performance gains which can be achieved by combining detectors, or their corresponding filter outputs, are considered.

Résumé

En octobre 2005, RDDC Atlantique a participé avec Centre de recherche sous-marine de l'OTAN (NURC) et GESMA (France) à un essai conjoint du véhicule semi submersible télécommandé DORADO. De nombreuses images d'objets de divers aspects, ressemblant à une mine et situés à diverses profondeurs, ont été prises sur le plancher océanique au moyen d'un sonar à balayage latéral. La position de ces mines factices est connue de manière très précise. Dans le rapport résumé ici, ces données sont utilisées pour étudier la performance de cinq algorithmes de détection. Le principe de chacun de ces algorithmes de détection est le résultat de certaines corrélations simples image filtre. Les statiques sur les objets détectés, les fausses alarmes et les cibles manquées sont présentées, ainsi qu'une analyse des statistiques sur les cibles manquées selon le type de cible et la profondeur à laquelle elle se trouve. La performance variable des détecteurs, évaluée d'après leur seuil de décision (courbes ROC) est aussi présentée. De plus, on examine des moyens d'améliorer la performance en combinant des détecteurs, ou leurs signaux filtrés.

This page intentionally left blank.

Executive summary

Computer-aided detection of targets from the CITADEL trial Klein sonar data

John A. Fawcett
Anna Crawford
David Hopkin, Vincent Myers, Benoit Zerr; DRDC Atlantic TM 2006-115; Defence
R&D Canada – Atlantic; August 2006.

Background

Computer-aided detection methods have an important role in sidescan sonar surveys, either as an aid to a human operator or for making detections during autonomous operations. During the CITADEL trial, an extensive set of Klein 5500 sonar imagery was collected for several dummy mine targets at a large variety of ranges and aspects. This data set is used in this report to statistically characterize the performance of 5 proposed automated detection methods.

Principal results

It was found that the computer-aided detection methods considered were able to detect all the types of targets with a high probability of detection (often 90% or higher), particularly for ranges between 20 and 50 m. However, the detectors showed a significant variation in the number of corresponding false alarms. The better methods were able to achieve the high detection rates with a fairly small false alarm rate in low clutter areas (for example, 1 false alarm/file or 55 false alarms/km^2, for targets in the ranges 15-55 m at the trial sites).

Significance of results

It is shown that realistic and stealthy mine shapes can be detected with a high degree of probability with a commercial-off-the-shelf sidescan sonar. The false alarm rates for a benign seabed can be made fairly small. The performances of the various detection methods depend upon the range of the target, the target type, and the background seabed characteristics.

Future work

In future work we would like to consider more sophisticated classification methods for the case where the clutter objects on the seabed are more minelike. Also, we

would like to consider the classification rates obtained after combining multi-aspect information for objects on the seabed.

Sommaire

Computer-aided detection of targets from the CITADEL trial Klein sonar data

John A. Fawcett
Anna Crawford
David Hopkin, Vincent Myers, Benoit Zerr; DRDC Atlantic TM 2006-115; R & D pour la défense Canada – Atlantique; August 2006.

Contexte

Les méthodes de détection assistées par ordinateur jouent un rôle important dans les études utilisant des sonars à balayage latéral, que ce soit pour assister les opérateurs ou pour détecter des objets au cours d'opérations autonomes. Pendant l'essai CITADEL, une série d'images détaillées de plusieurs mines fictives ont été prises avec le sonar Klein 5500 ; l'aspect de ses mines de même que la profondeur à laquelle elles se trouvaient variaient. Cet ensemble de données est utilisé dans le rapport résumé ici pour caractériser, au moyen de statistiques, la performance de cinq méthodes de détection automatisées proposées.

Résultats

Les méthodes de détection assistée par ordinateur examinées ont permis de détecter tous les types de cibles et ce, avec une probabilité de détection élevée (souvent d'au moins 90%), en particulier dans une plage de profondeurs comprises entre 20 et 50 m. Toutefois, le nombre de fausses alarmes pour chacun des détecteurs variait considérablement. Les meilleures méthodes permettaient d'obtenir des taux de détection élevés avec un taux de fausse alarme relativement faible dans les zones de faible fouillis radar (par exemple, une fausse alarme/un fichier de fausse alarme ou 55 fausses alarmes/km^2, pour des cibles se trouvant à des profondeurs de 15 à 55 m sur les sites des essais).

Portée

Il a été démontré que les formes de mines réalistes et furtives peuvent être détectées avec une grande probabilité au moyen d'un sonar á balayage d'ondes commercial. Le taux de fausses alarmes pour un plancher océanique lisse peut être grandement réduit. La performance des diverses méthodes de détection dépend de la profondeur de la cible, du type de cible et des caractéristiques du plancher océanique à l'arrière plan.

Recherches Futures

Dans les recherches futures, nous aimerions examiner des méthodes de classement perfectionnées pouvant être utilisées dans les cas où des objets situés dans un fouillis radar sur le plancher océanique ressemblent beaucoup à des mines. Nous aimerions aussi nous pencher sur les taux de classements obtenus après avoir combiné des données sur de multiples aspects d'objets se trouvant sur le plancher océanique.

Table of contents

List of figures

1 INTRODUCTION

Over the last 5 years DRDC Atlantic has collected a large number of sidescan sonar images of replica mines (which we will refer to as targets in this report) placed upon the seabed at different locales. The sidescan sonar used in these trials was a Klein 5500 sidescan sonar. This sonar was used as the sonar for the Remote Minehunting System (RMS) Technology Demonstration Project. In this case it was attached to the Aurora towfish and deployed from the remote vehicle DORADO. In the past, a database of sidescan sonar images for a number of targets and non-targets (e.g., rocks, scour marks, etc.) was formed by manually extracting small segments of sonar data (swaths) that were deemed to correspond either to known targets or non-targets of interest. These images have been used to study automated classification methods [1] and human operator performance [2]. For a totally computer-automated detection/classification system, the initial determination of the sonar swaths of interest should also be done by the computer. One can envision a two-level detection/classification stage, where the first stage consists of a fairly simple detection method which identifies a fairly large number of regions of interest and then a more sophisticated second stage which analyzes these regions in more detail. The hope is, of course, that the first detection stage will not miss many targets but also will not detect an inordinate number of false alarms. In this report we will investigate 4 basic detectors which can be implemented as two-dimensional cross-correlations of the sidescan sonar image with filters. In addition, a detection method provided by NURC is also implemented.

During October 2005 DRDC Atlantic, NURC, and GESMA (France) participated in a joint MCM trial at locations near La Spezia, Italy. The DORADO/Klein 5500 system was used with vehicle control and real time data collection and display aboard the NURC vessel, CRV Leonardo. We will consider 2 sites where dummy targets were deployed. The positions of the targets on the seabed are accurately known: their GPS positions were noted at the time of deployment and Reson 8125 multibeam bathymetric surveys of the target regions also yielded very accurate positions. Using these positions of the targets we can estimate (computer-automated) the number of correct target classifications, the number of false alarms (detections which are too far from any known target position) and missed targets (targets whose position is predicted to lie within a sonar file and are not detected). These performance statistics can be analyzed as a function of the detector. As well, the missed target statistics can be analyzed as a function of target type, target range, and target aspect. We will also consider combining the various filter output levels. It is hoped that such a combination will yield another detection method with a high detection and low false alarm rate.

2 DATA PROCESSING

A MATLAB code was written to read in individual Klein 5500 sidescan sonar files. In the case of the files being written out by the RMS software, each file contains 501 pings of data (with 5 starboard and 5 port beams). The sonar was run with the 75-m setting and the along-track resolution is nominally 10 cm. The data is first reduced to the "visible" beams by using the visible beam indices specified in the Klein ping header. Only the across-track indices from 301 (corresponding to approximately 10 m in slant range) to 2274 are used (for both port and starboard sides) The data is then decimated by a factor of 3 in the across-track direction by using a 3-point median filter. This is done to reduce the amount of data being processed. It also makes the pixels approximately square, as in the unreduced format, a pixel represents a 10 cm x 3.3 cm area. This data set is then normalized in the across-track direction by computing individually for the port and starboard sides a mean across-track amplitude curve. The data is then divided by this curve to reduce the overall amplitude variation of the data with respect to the cross-range. Each file (and side) is normalized by its own individual normalization curve.

There are 4 different detectors we initially consider for these data sets. They all utilize the outputs from convolving the data with specified filters. Some of them involve the ratio of outputs from 2 different filters. It is hoped that by being able to formulate the detector in terms of filter convolutions, that the processing can be made relatively efficient. A fifth detection method was provided by NURC. In this case, the original Klein files were preprocessed to form bitmap files and these files were then processed by a C-executable to form filtered images. These images, once thresholded provided the detections. We read these filtered images into our MATLAB routine and then treated the detection regions in the same fashion as the results from the other detection methods. The details of the implemented detectors are now described. We will consider 2 sets of parameters for each of the detectors.

2.1 Detector 1

One of the basic type of detector filters has been discussed by Dobeck at al [3]. Its basic concept is to consider a target as composed of a few rows (along-track direction) and columns of highlight pixels (values at the high end of the histogram) and a few rows and some columns of shadow pixels (values at the low end of the histogram). It is hoped that by match-filtering the data with a two-dimensional filter, which qualitatively approximates a "generic" target image, target-like features will be enhanced in the output filtered space and more easily detectable. We actually use 3 different filters depending upon the cross-range of the data. The first two-dimensional filter is 4 x 9 with the first 4 columns having the value +1 and the last 5 columns having the value -1. The second filter is 4 x 14 with the first 4 columns

having the value +2 and the last 10 columns having the value -1. The third filter is 4 x 19 in size with the first 4 columns having the value +2 and the last 15 columns having the value -1. For all these 3 filters, the filter is normalized so that the sum of its absolute values is equal to unity. These 3 filters are shown in Figs.1a-1c. Before cross-correlating these filters with the sidescan sonar data, the data is preprocessed. The median value of the data is subtracted from the data, so that data values less than the median are negative and values greater than the median are positive. In this manner, when the data values have a structure similar to a hypothesized target, in terms of high/low values, the cross-correlation between the data and the filters should be high.

As outlined above, 3 different filters with the data are used. This is because the acoustic shadow which is cast by an object on the seabed increases with increasing cross-range. For example, for a towfish altitude of 10 m, an object 0.5 m high will have shadow lengths of 7.5/9.5 m (8 10-cm pixels), 15./9.5 m (16 pixels), and 22.5/9.5 m (24 pixels) at cross-ranges of 15,30, and 45 m respectively. In theory, it would be desirous to cross-correlate the data with a filter whose shadow length increases continuously with cross-range. However, for computational efficiency we chose instead to use 3 standard two-dimensional cross-correlations with the 3 filters discussed above. A hybrid filtered image is then formed by using the output from the small filter, medium-sized filter and large filter for approximate ranges: (a) 9.9 - 22.75 m, 22.75 m - 50 m, and 50 m -75 m or (b) 9.9 - 30 m, 30 m - 59.4 m, 59.4 m - 75 m. The second set of ranges corresponds to using smaller highlight/target filters to further ranges. In fact, in our analysis of detections we will not consider detections further than 59.4 m so that effectively we do not consider the outputs from the third two-dimensional filter in this case.

We use a two-dimensional convolution function from MATLAB (convolution and correlation are essentially the same with a reverse in the direction of the filter) to carry out the filtering. One technical problem with this approach is that the output values of the filter near the edges of the grid are, in general, less than they should be, due to the data being zero-padded for the two-dimensional convolution. This is a concern for all the detectors described in this report.

One problem with simply using the thresholded values of the output image as a detector is the case of a large, extended clutter object, such as a log, a scour, a cable, etc. where one will simply have a long sequence of connected detections. We will use a region-labelling method to group such detections into clusters, so that these cases could be ruled out on the basis of being too long in the along-track direction. However, in order to reduce the number of initial detections immediately, we can normalize the output image in such a way that if the surrounding background has an overall high level in terms of the statistic of interest, then the output value will be

diminished. We do this in the following manner,

$$O(x,y) = \frac{\hat{O}(x,y)}{\mu(1 + .5\gamma(x,y)/\mu))} \quad (1)$$

where $\hat{O}(x,y)$ denotes the filtered image (using the appropriate range value definition as discussed above), μ is defined as the median value of the positive values of $\hat{O}(x,y)$ and $\gamma(x,y)$ is a sliding average of the positive values of $\hat{O}(x,y)$ over a 50 (along-track) x 5 window. Here we use $'x'$ to denote the along-track coordinate and $'y'$ for the across-track coordinate. The normalization of Eq.(1) results in high output levels being diminished if the average value over a 5-m along-track average is also relatively high. For this and the other detection methods, the filter outputs are often considered relative to an estimate of a background level. In this manner, it is hoped that the results will be robust to the levels of the sonar return.

The value of $O(x,y)$ is thresholded at a value of 7.5 (with a resulting image of ones and zeros). This image is expanded using a small square filter and this resulting image grouped into connected regions. The centres of these regions are defined as the detections. The threshold values that are used for the detectors of this report are somewhat arbitrary. They were chosen to detect most of the targets but often produce several false alarms/file. However, the maximum or minimum output values of the various filters within the initial detection regions are saved in a file. Thus, the effect of varying the threshold value on the number of detections and false alarms can be subsequently examined.

2.2   Detector 2

A second detection statistic we consider is the image lacunarity. The image lacunarity as an object detector was discussed by Kessel in Refs. 4 and 5. The lacunarity is defined as

$$\ell(x,y) = \frac{\sigma^2(x,y)}{m(x,y)^2} \quad (2)$$

where $\sigma(x,y)$ denotes the standard deviation at the point (x,y) and $m(x,y)$ is the mean. These values are computed using a sliding window over the image values. The dimensions of the windows we use for this are the same as the filters described for Detector 1 and for the same 2 sets of range intervals. In this report, a value of 1.0 was used for the initial threshold. As before the thresholded image is expanded and then grouped into regions. The centres of these regions are used to define the detections. It was originally found that there were often many false alarms along the line of the first across-track pixels; this was probably due to the computed value of $m(x,y)$ being abnormally small (as discussed, the filter computations will be misleading near the edges of the grid). To avoid this problem, the mean $m(x,y)$ was set to a very high

value for indices near the edges of the grid (4 points for first across-track indices, 9 points for the last across-track indices, 3 points at the top (along-track) and 4 points at the bottom of the grid).

2.3   Detector 3

A third detection method is based upon the approach described in Ref.6. It detects objects on the basis of the acoustic shadows. In particular, we use the value

$$\Gamma(x, y) \equiv 20 \log_{10}(\frac{m_1(x, y)}{m_2(x, y)}) \tag{3}$$

where $m_1(x, y)$ is the averaged value over a sliding window. Once again, we use 3 different windows in the computation of $m_1(x, y)$ for the 2 different sets of cross-ranges. We considered 2 different sets of parameters for the filters. For the first set of parameters, the sizes of the 3 filters are those of the shadow size used in the 3 filters of Detector 1; 4×5, 4×10 and 4×15. The value $m_2(x, y)$ is defined over a larger region by using a large window. Here we use a window which is 50 x 50 in size. However, only the outer edges of width 10 pixels are used; the centre region is zero thereby excluding the region covered by the smaller windows in the computation of $m_1(x, y)$. This filter is shown is Fig.1d. Second, we considered the second set of range intervals for the hybrid output. In this case, the filter sizes were 4×4, 4×7, and 4×12. The background filter in this case taken to be 40×40 with all ones. This second set of filter parameters uses smaller shadow regions for a given range than does the first set of parameters. The motivation behind this was to attempt to improve the detection rate for some of the smaller targets. For the second set of range intervals, the third interval is not considered in the analysis of detections, so that in this case only the first 2 shadow filters are relevant. We use an initial detection threshold of -4.5 for the 2 sets of filter/range parameters.

2.4   Detector 4

The fourth detection method is a variation of the first detector. However, instead of using the image values directly, the image values are first redefined as one of 5 values: (1) deep shadow values are assigned the value -1 (2) shadow values are assigned the value -0.5 (3) highlight values are assigned the value +0.5 (4) high highlight values are assigned the value +1 and (5) all other values are assigned the value zero. The thresholds which specify deep shadow,shadow, highlight and high highlight are defined in terms of the median image value μ. In particular, deep shadow is defined as less than $0.3 \times \mu$, shadow $0.6 \times \mu$, highlight is defined as greater than $2 \times \mu$ and high highlight is greater than $4 \times \mu$. This new set of image values $I_n(x, y)$ (i.e., -1,

-0.5, 0., 0.5 and 1) are convolved with the same filters as with detector 1 to yield the filtered image, $\hat{\Omega}(x, y)$. The values of $\hat{\Omega}(x, y)$ are then normalized by

$$\Omega(x, y) = \frac{\hat{\Omega}(x, y)}{1 + 10N(x, y)} \tag{4}$$

The normalizing filter $N(x, y)$ is the average absolute value over a 50x5 window of $I_n(x, y)$. Thus in the regions where there are extended regions of highlight and shadow values the output is penalized. Once again we consider the 2 sets of range intervals for the definition of our hybrid filter results. For the initial threshold in the computations we use $\Omega(x, y) \geq 0.15$.

2.5 Detector 5

The fifth detector is the one provided by NURC. It is based upon the work of Petillot et al [7]. The algorithm applies a non-linear window technique to search for areas of highlight and shadow. The window is adjusted in range to compensate for the lengthening of the shadow in slant range depending on the size of the objected being detected. A Z-test is performed on the means of the pixel gray levels within and outside the window area, a detection being called when the test statistic exceeds a certain threshold. As discussed previously, the Klein files are preprocessed first outside of the main MATLAB code, the filtered image files are read by the MATLAB code, thresholded and the detection regions treated in the same fashion as our other methods. There is a parameter for the filtering stage which defines the minimum height of the object to be detected. We will consider this value set to either 25 for filter parameter Set 1 or 35 cm for the second set of parameters. In both cases, the initial threshold level was set to three.
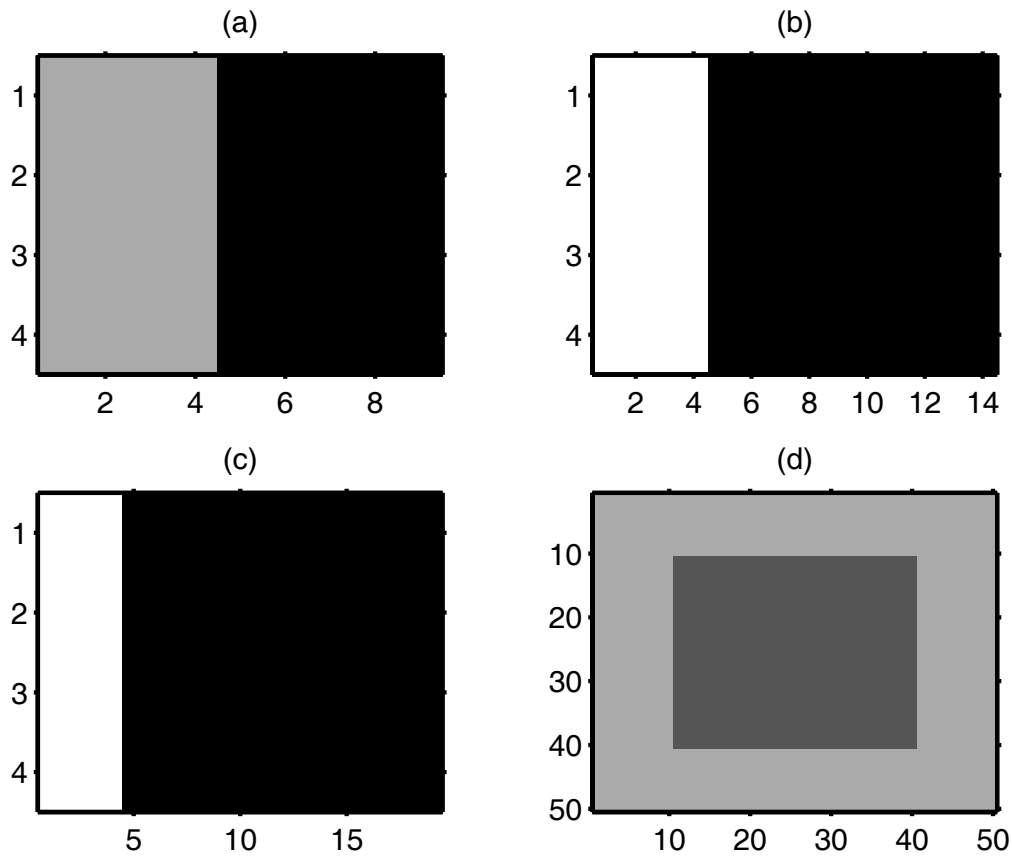
Figure 1: *Four of the filter (windows) used in the computations: (a) the short-range filter for Detectors 1,2, and 4 (b) the medium range filter (c) the long range filter (d) one of the large background filters used for the relative shadow computations of detector 3 - the interior of this filter had the value zero.*

3 DETERMINATION OF VALID DETECTIONS, FALSE ALARMS, AND MISSED TARGETS

As discussed in the previous section, a sequence of Klein sonar files are read in and processed with different filters for the 5 detectors. A set of detections is then made for each detector. The port and starboard sides are processed independently. Using the range of a detection, the towfish altitude, and heading and longitude and latitude of the towfish (as recorded in the Klein file header) the detection indices are converted to Eastings and Northings coordinates. The positions of the deployed targets, as estimated from the Reson bathymetric survey, are then compared to the detection positions. We only consider detections that are at least 3 m, in slant range, greater than the maximum altitude during the file. The detection must also be less than 59.4 m in range. The along-track position must be greater than 2 m from the start and end of the file. Within these constraints, it can be determined if there is any deployed target within 7 m of this detection. For the case, where this is true, the detection is declared as a target detection. Otherwise, it is declared a false alarm.

There is also the very important issue of targets which are present in a file and which are not detected. To estimate these target "misses", we consider those targets which are assumed to lie between 3 m greater than the maximum altitude and 59.4 m and also greater than approximately 4 m and 5 m in the along-track direction from the start and end of the file. If there are no detections (within the constraints discussed above for detections) then a target is declared as missed.

All the detections and missed targets and additional associated information are stored in a large file which summarizes the processing of all the requested files. In the post processing of this file, we further refine our logic with respect to estimating the target detections and misses. For each file, the detections and misses for the various target types are entries in the detection and missed target matrices, where the matrices are 5 (number of methods) × 10 (number of targets for Massa site). The elements of this matrix are one for a missed target (for the "misses" matrix) or detection of a target (detection matrix). The port and starboard detections and misses are combined into 1 matrix. There are instances, for a given detector, where a target is detected more than once by a detector. This can occur if there are 2 distinct regions after thresholding, if there is a multipath image of the target, or at the longer ranges, if the towfish motion (particularly, heading variation) causes the same target to appear more than once. The described matrix method only counts these multiple detections once. Thus, we compile estimates of the detections and misses for each target type, detection method, and file. We can sum the results with respect to the file index to get statistics for the entire data set considered.

From the previous discussions, it is clear that the detection and missed statistics

for the short range targets (slant ranges less than 15 m) are a little suspect. The detections and predicted target positions are not considered below a minimum range (dependant upon the altitude) and we only processed data greater than about 9.9 m (slant range). The output of the filters become inaccurate towards the edges of the grid due to the zero-padding of the cross-correlation process.

In the next section, we will compute the probability of detection as a function of slant range. The histogram of this quantity is computed in the following manner. We first compute the histogram of the detections, with specified range bin centres ($i = 1, ..., N$), yielding $D(r_i)$. Similarly, we compute the misses histogram $M(r_i)$. The probability of detection distribution is then computed from

$$p(r_i) = \frac{D(r_i)}{D(r_i) + M(r_i)}. \tag{5}$$

For the initial detection/miss results we attempted to obtain a high rate of detection. For some of the methods, there was quite a high false alarm rate associated with this. However, the maximum (or minimum values) of the output filters within the detection regions for both targets and clutter were saved. Thus, subsequently, we can change the threshold and determine whether a target would be "missed" and false alarm which would be eliminated. In this way, we can obtain an estimate of a ROC curve.

4   RESULTS

In this section we will summarize the results of using the 5 detectors discussed in the previous section in terms of missed targets, number of detections, and the number of false alarms. There were 2 targets areas considered: Area D off Marina di Massa and Area E, off Levanto. In both cases, the bottom produced a rather weak sonar return and there were noise issues with the sonar at ranges greater than approximately 50 m. The bottoms were very benign, however, in terms of clutter. The Rhib boat which was used to accompany the DORADO did sometimes produce a wake which was observable in the sonar image and this feature could cause false alarms. On some occasions, the data was recorded during the transit out to the target sites. The data near the pier at NURC and on the way out of La Spezia harbour was cluttered with various rocks, man-made objects and scours. Thus, this data was useful in providing a test of the number of false alarms in a cluttered region. Since, none of the detections in this region correspond to the deployed targets, they are, by definition, "false alarms". However, it should be noted that some of the detections do correspond to objects which are minelike. At various times during the trial, the DORADO came to a stop in order to avoid boats, flotsam, etc. The Klein files, corresponding to these times, were not included in the list of files to process.

4.1   Area D

There were 10 objects deployed on the seabed. Only 7 of them were, in fact, minelike objects. One of the objects was a rock (an often-used NURC rock), one of the objects was a gym bag stuffed with rubber, and another object was a "wedding cake" object, consisting of a stack of plateaus of different diameter. Thus, it is not clear whether the automated detection of these non-minelike objects is desirous or not; however, we will consider them all as targets. The other targets consisted of minelike shapes: a cylindrical shape, and 3 other shapes which we will denote as A,B, and C. This site was visited on 4 different days after the targets had been deployed. We will consider the data from 2 of these days, October 24 and 26 when a large number of multi-aspect runs were made with the RMS system. The detection and missed statistics are shown below, combining the results from days 24 and day 26. For all the targets, excepting the wedding cake, the estimated number of possible target detections ranged from 87 for target C to 102 for one of the 2 instances of target B.

The initial detections/false alarms for the various methods were initially made with thresholds which were set low to yield high detection/false alarm rates. However, as discussed, the maximum (or minimum) values for the filtered images in the regions of the initial detections regions are recorded. Then in post-processing one can change the threshold levels and determine which target and false alarm detections remain. In this manner Receiver-Operating-Characteristic (ROC) curves can be computed. In
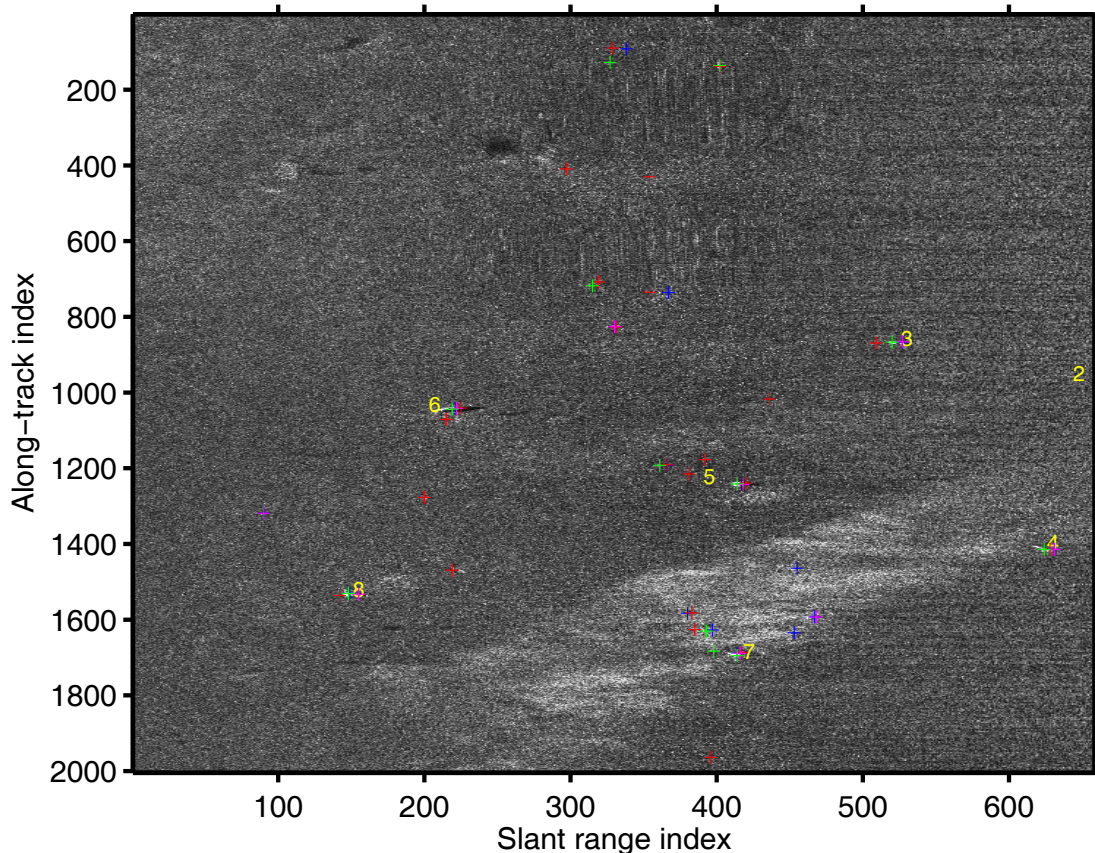
Figure 2: *A representative sonar image from the target site - the target locations are indicated by a red number. The detections from Method 1 are shown as in blue, Method 2, red, Method 4, maroon and Method 5, green*

Fig. 2 we show a representative image from October 24. The predicted locations of some of the targets are indicated by a yellow numeral and the detections of 4 methods 1,2,4,and 5 (for their initial detection threshold values) are shown as plus symbols with different colours. As can be seen, all the methods have detected most of the various targets. There are also a number of false alarms (i.e., detections which do not correspond to one of the target locations) and it is clear that these false alarms vary with the detection method. In Fig. 3 we show a "zoom" of Fig. 2 about one of the cylinders. All of the methods have detected this cylinder.

In Fig.4 we show ROC curves for the 5 methods using the data from October 24 and 26 for the 2 different sets of parameters. These are for the detections and misses which lie within the ranges 15-55 m. As can be seen from Fig. 4, the detection rates for 4 of the methods are high with low false alarm rates with methods 1,4, and 5 having the best overall performance. The performance of Method 3 noticeably improves when the second set of parameters, corresponding to small filter sizes for the shadow and a

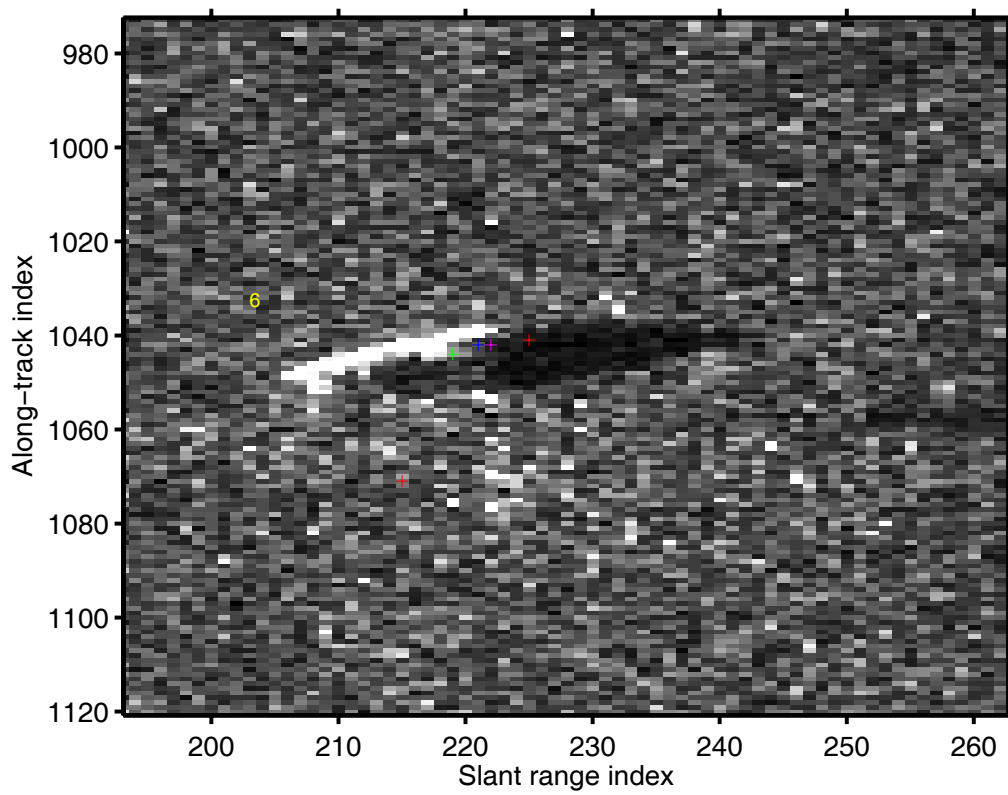**Figure 3:** *A zoom of the region about a cylinder in Fig. 2*
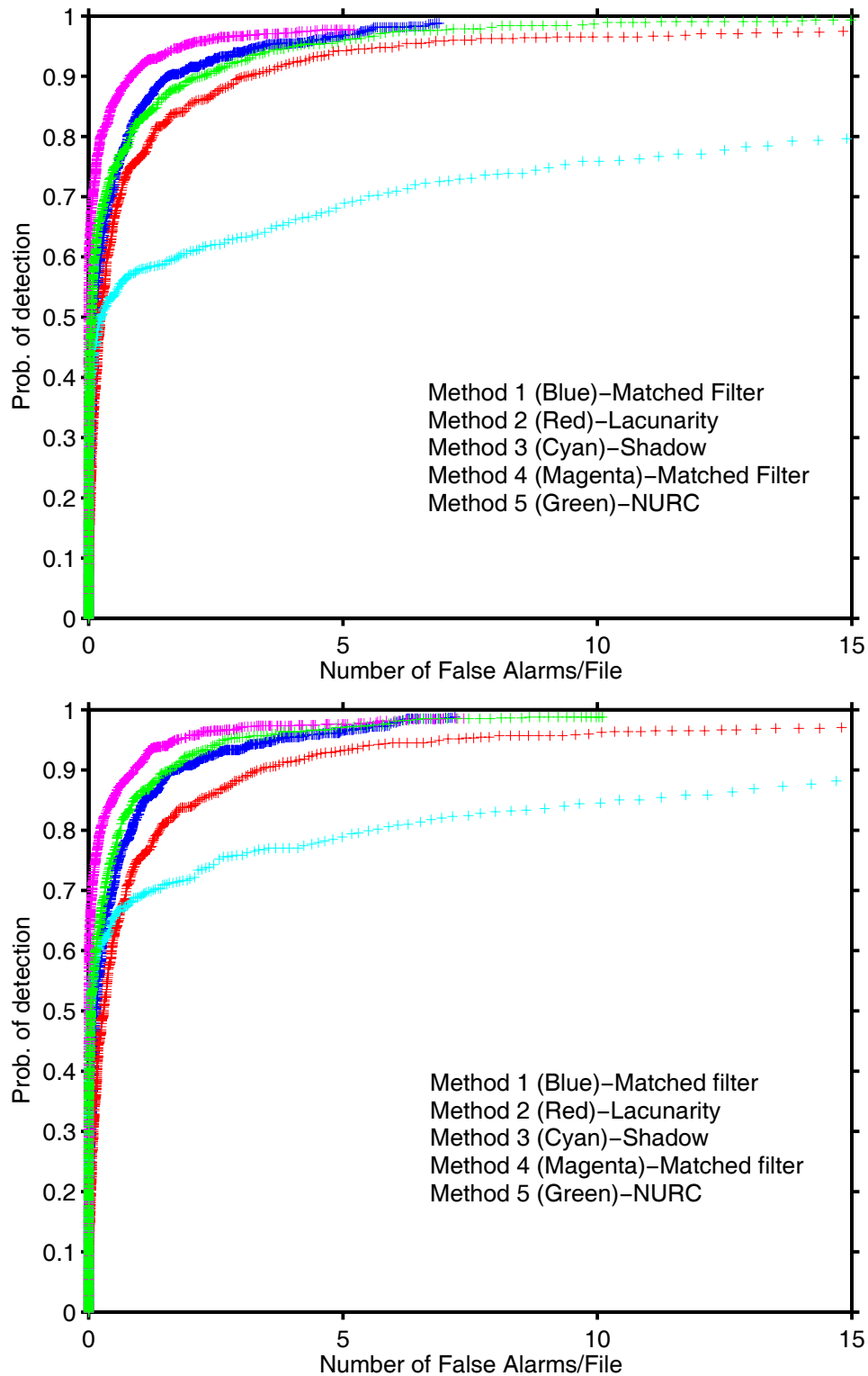
Figure 4: *The ROC curves for October 24-26 for the Detection Methods and the 2 sets of parameters. Only detections and misses in the slant range interval [15m 55m] are considered.*

simple 40×40 box for the background is used. For the other detectors, there is not a significant difference in the appearance of the ROC Curves for the 2 sets of filter parameters. In this figure, the false alarm rate is specified in terms of number per file. Each file corresponds to about 55 seconds and thus the rate per second can be easily obtained for these curves. The sonar moves approximately 220 m along-track in a file and if we consider the across-track swath of 40 m (twice this for the 2 sides), we obtain an approximate coverage rate of $(.22 \times .08)$ km^2 per file. Thus 1 false alarm per file would correspond approximately to 55 false alarms/km^2.

We can also consider the performance of the detectors as a function of range (Fig. 5). In this case we consider the thresholds for the detectors to be set at the value which yields one false alarm/file. The curves are, in general, as one would expect. There is an increase in the probability of detection as the range increases and a slight decrease at the further ranges. This decrease is most noticeable for Method 3. One should recall that in fact we only consider detections out to approximately 60 m range so that the statistics will tend to be less reliable at 55 and 60 m.

We can also examine the detection performance of the methods as a function of the target type. In Tables 1 and 2 we show the detection rates against the 10 targets for false alarm rates of 1 and 2 per file and for the 2 sets of filter parameters. All methods performed well with respect to the cylinders and target type A. The targets for which the methods had the poorest performance were target types B and C. Methods 1 and 4 performed well with respect to the target type B, particularly for the false alarm rate of 2 per file. Method 5 had some detection problems with the second instance of target type B. Methods 4 and 5 also had some detection problems with respect to target type C, while Methods 1 and 2 performed very well with respect to this target. Table 2 shows the same results but for the second set of parameters for the various methods. The detection rates are approximately the same with the exception of Method 3 which is significantly better for the second set of parameters (recall, smaller shadow filter sizes and a different filter for the background level). It should also be emphasized that the detection rates are for specified false alarm rates. As indicated by the ROC curves, the methods can detect the targets at greater probabilities than those shown in the tables but at the expense of more false alarms.

Although, the methods of this report have high detection rates and low false alarm rate, it is important to note that the seabed environment at the sites is quite un-cluttered. Many of the false alarms are caused by wake, fish, and various random highlights and shadows. It is interesting to consider the false alarm rates for the various methods when the DORADO is exiting La Spezia harbour from the NURC pier. Since no known targets were deployed in this region, all detections are, by definition, false alarms. This region has considerably more clutter and scours than the trial sites. In Table 3, the number of detections/file made by the 5 methods are given for the 2 sets of parameters. The thresholds for the methods were set to
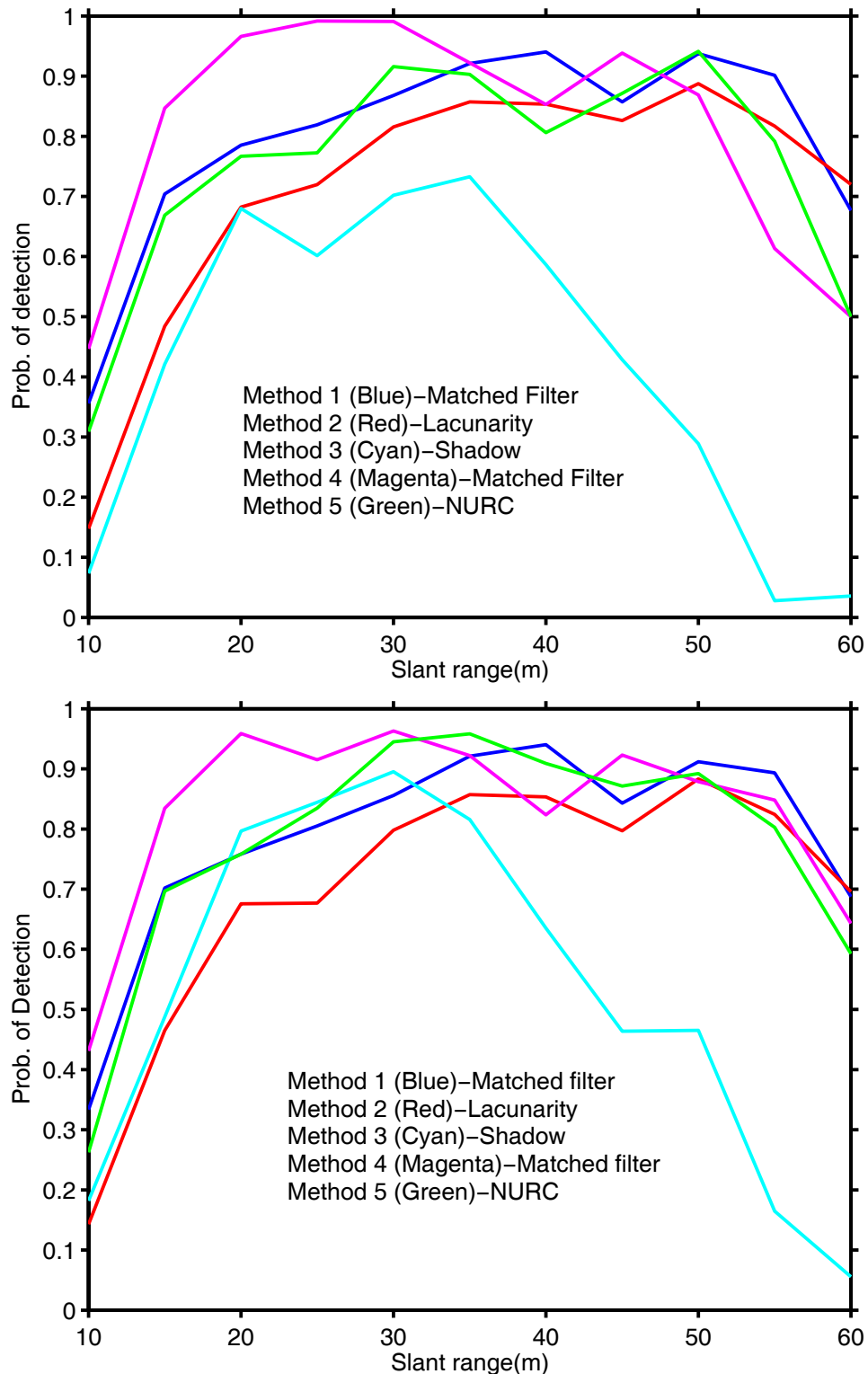
Figure 5: *Probability of detection versus slant range for the 5 methods for thresholds set to produce one false alarm/file - Site D. The top graph is for the first parameter set for each of the methods and the bottom graph is for the second set of parameters.*

Target	Method 1		Method 2		Method 3		Method 4		Method 5	
Cylinder 1	89	89	93	99	86	89	96	97	96	99
Cylinder 2	74	85	79	93	89	90	99	99	95	99
B1	60	81	35	51	31	37	93	96	73	84
B2	62	81	41	56	23	26	81	92	53	64
Gym Bag	85	93	71	81	36	42	90	93	88	93
Rock	99	99	98	99	88	88	99	99	100	100
A1	95	99	91	96	79	80	98	99	96	96
A2	95	99	82	90	72	73	96	98	98	99
C	96	97	95	99	27	55	68	82	37	65
Wedding Cake	97	97	93	93	54	69	97	100	94	97

Table 1: *Detection probabilities for the deployed targets - Site D - (when the target is estimated to be 15-55 m slant range from sonar)for the 5 methods. For each method the rate is shown for the thresholds set to produce 1 false alarm/file and 2 false alarms/file. Thus, for example, the first column for Method 1 gives the detection probabilities for a false alarm rate of 1 per file and the second column gives the values for 2 false alarms per file. The first set of range and filter parameters are used.*

Target	Method 1		Method 2		Method 3		Method 4		Method 5	
Cylinder 1	87	89	90	96	88	88	97	99	95	98
Cylinder 2	73	83	74	90	88	89	98	99	98	100
B1	58	78	35	47	63	71	94	96	77	91
B2	57	77	41	55	51	54	82	94	56	64
Gym Bag	83	92	67	82	57	63	92	95	83	92
Rock	99	99	96	99	92	94	98	99	98	100
A1	95	99	91	96	78	80	99	99	99	99
A2	96	100	80	89	79	83	96	96	99	99
C	96	99	93	99	70	85	58	82	60	85
Wedding Cake	97	97	93	93	82	85	100	100	97	100

Table 2: *Detection probabilities for the deployed targets - Site D -(when the target is estimated to be 15-55 m slant range from sonar)for the 5 methods. For each method the rate is shown for the thresholds set to produce 1 false alarm/file and 2 false alarms/file. The second set of range and filter parameters are used.*

Method	Detections/File - Set 1	Detections/File - Set 2
1	1.42	1.53
2	1.79	1.95
3	13.84	21.1
4	16.73	17.63
5	5.53	2.79

Table 3: *The number of detections/file lying within the ranges 15-55 m for the first 19 files exiting La Spezia harbour (October 24, 2005) . The thresholds for the various methods are set to those which produced 1 false alarm/file at Site D. The results for the 2 sets of filter parameters are shown.*

the values which produced one false alarm/file at Site D. As can be seen, there is a significant increase in the number of detections/file, particularly for Methods 3 and 4 and somewhat for Method 5. This does not mean that, for example, Method 4 is no longer a good detector. It is more an indicator that the ROC curve may change from one environment to another. In Fig. 6 we show the portside image for one of the files with the detections of Methods 1,2,4,and 5 indicated by blue, red, magenta, and green '+' markers respectively. There are a number of detections from Method 4 (magenta) and few, if any, from the other methods. However, a detailed examination (Fig. 7) of some of the detections in Fig. 6 indicated that some of them are very reasonable. Hence, although the threshold for Method 4 may be set a little low for this environment, the other methods may, in fact, require a lower threshold.

4.2 Site E

On October 25 Site E, which was located off Monasteroli, was surveyed. In this case there were 7 targets deployed: 2 cylinders, 2 A-type targets, 2 B-type targets and a rock. There are less target acquisitions than for site D; on average, about 33 looks at each target. In Fig.8 we show the ROC Curves for the methods and 2 sets of parameters and in Fig. 9 the probability of detection/range for a false alarm rate of one per/file. The ROC Curves are quite similar to those of Fig. 4 for Site D, although a lower initial threshold should probably have been used for some of the methods as their ROC curves start at quite low false alarm rate values. The overall detection rates are somewhat lower for this site with a highest value of about 95%. Once again Method 3 performs better with the second set of filter parameters. The probability of detection/range curves of Fig. 9 are similar to those of Fig. 5, with the exception of Method 3 in the lower plot(the second set of filter parameters). For this site, Method 3 shows good performance out to 50 m.

In Tables 4 (filter/range parameter set 1) and 5 (filter/range parameter set 2) we examine the detection performance for the various targets. These rates are shown in
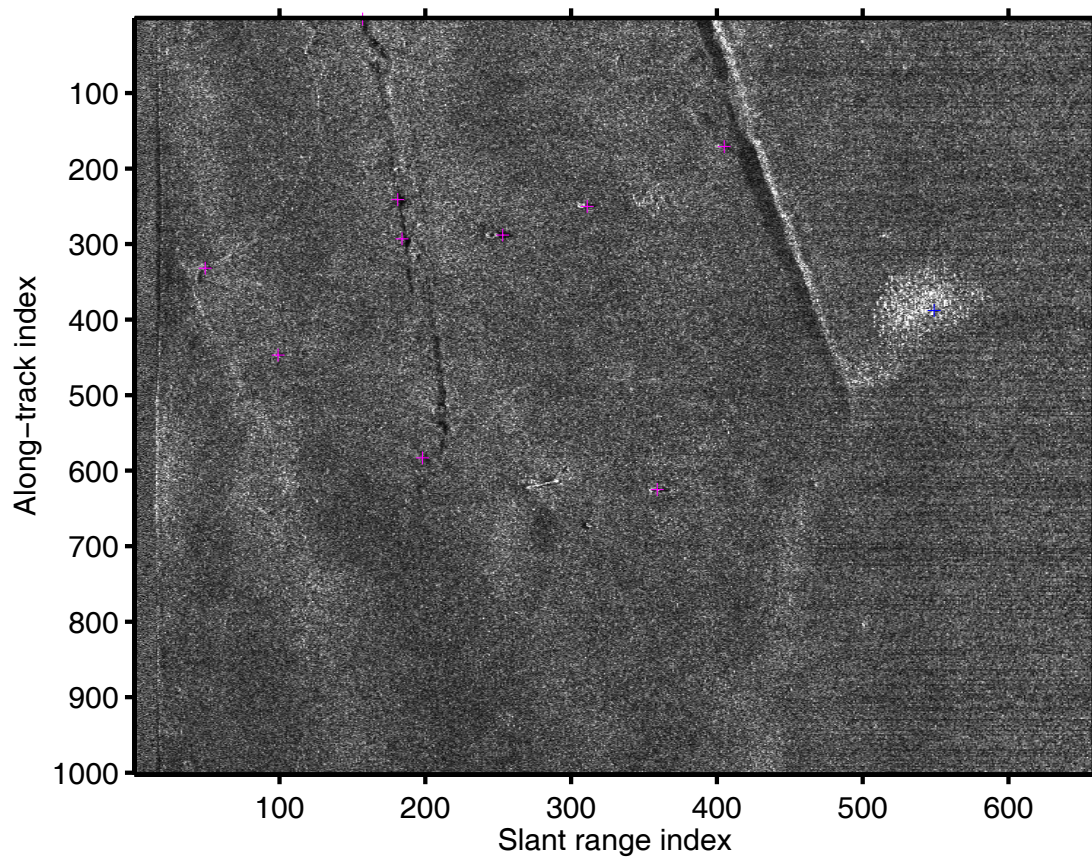
Figure 6: *A representative sonar image from transit out of La Spezia. The detections from Detector 1 are shown as a blue '+', Detector 2 a red '+', Detector 4 a magneta '+' and Detector 5 a green '+'*
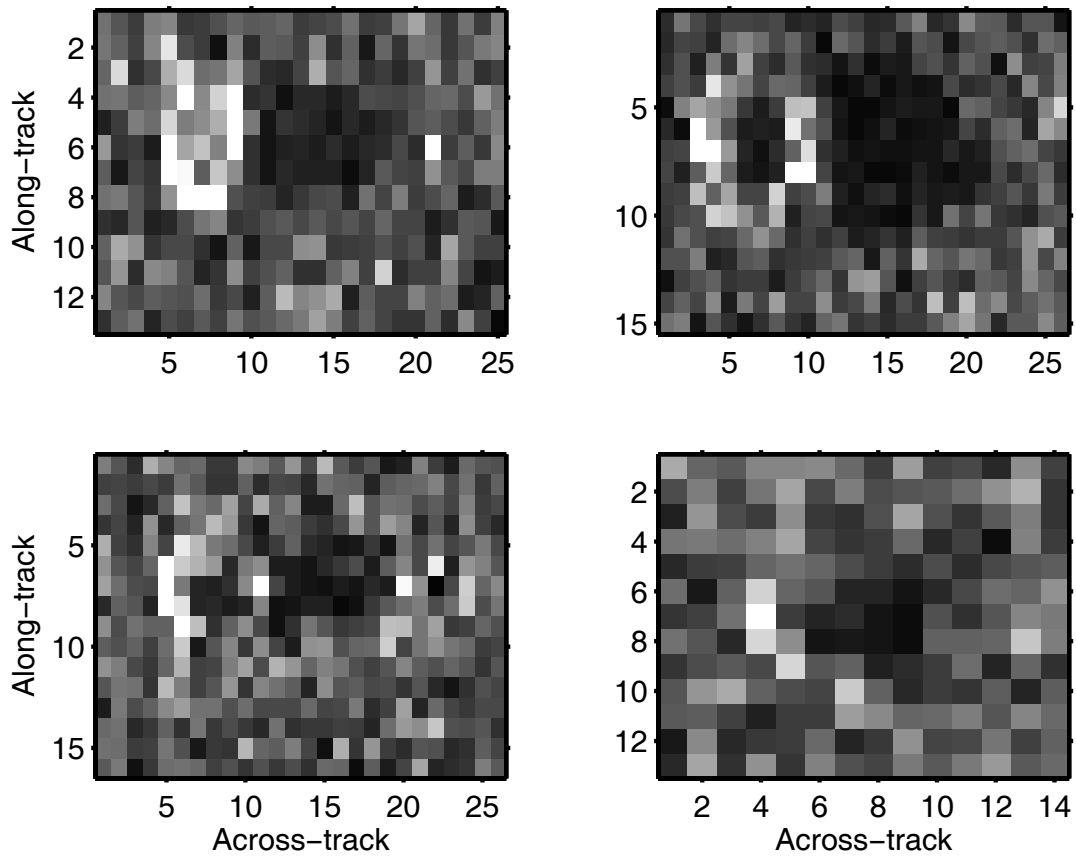
Figure 7: *Four images from Fig. 6 where Method 4 made a detection.*

Target	Method 1		Method 2		Method 3		Method 4		Method 5	
Cylinder 1	62	92	80	88	96	96	96	96	86	89
Cylinder 2	87	97	97	97	97	97	97	97	97	97
B1	54	76	39	66	21	21	81	86	49	65
B2	44	72	52	68	37	37	88	91	66	88
Rock	94	97	94	94	87	90	97	97	97	97
A1	91	95	95	95	76	81	95	95	95	95
A2	64	77	73	73	68	73	76	81	77	77

Table 4: *Detection probabilities for the deployed targets - Site E - (when the target is estimated to be 15-55 m slant range from sonar)for the 5 methods. For each method the rate is shown for the thresholds set to produce 1 false alarm/file and 2 false alarms/file. The first set of range and filter parameters are used.*

Target	Method 1		Method 2		Method 3		Method 4		Method 5	
Cylinder 1	65	92	80	84	92	96	96	96	88	96
Cylinder 2	87	97	97	100	100	100	97	97	97	97
B1	51	73	37	66	62	62	89	94	49	62
B2	35	74	48	68	58	61	88	91	75	90
Rock	94	97	90	94	88	88	97	97	97	97
A1	94	97	95	95	86	90	95	95	95	95
A2	64	77	73	73	78	83	76	76	77	77

Table 5: *Detection probabilities for the deployed targets - Site E - (when the target is estimated to be 15-55 m slant range from sonar)for the 5 methods. For each method the rate is shown for the thresholds set to produce 1 false alarm/file and 2 false alarms/file. The second set of range and filter parameters are used.*

the 2 columns for the thresholds set for the detection methods to yield 1 and 2 false alarms/file. As can be seen, the detection rates for Method 4 are high for all targets with the exception of the second instance of target type A where its rate is between 76 and 81% (and this target was problematic for all the methods). The performance of Method 5 is also good although its detection of the first B-type target is a little low at 65% for the first set of parameters and a false alarm rate of 2 false alarms/file. Also, Method 3 performs much better with the second set of parameters and only has problems with the detection of target type B (and even these are detected at about 60%).
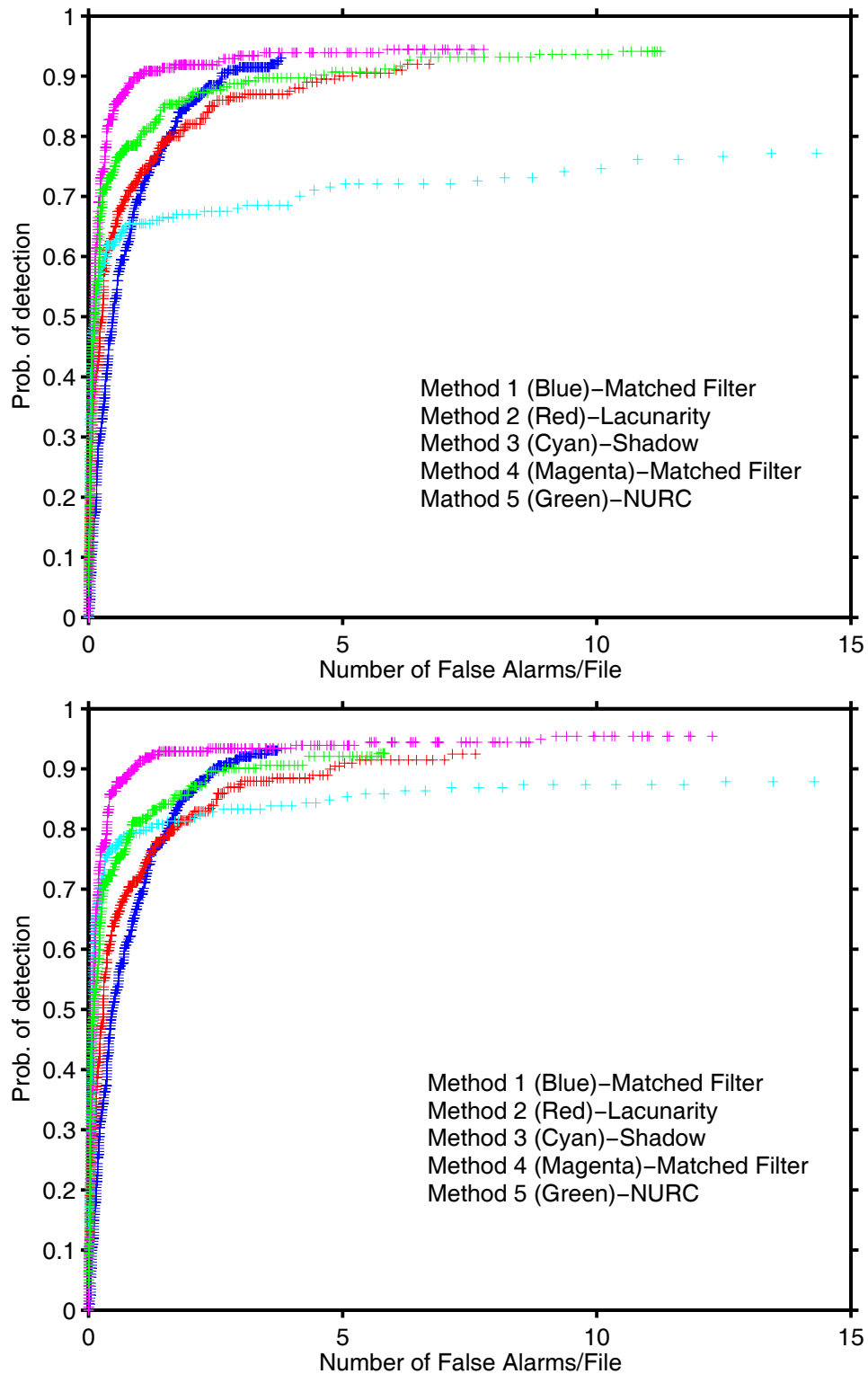
Figure 8: *The ROC curves for October 25 - Site E - for the Detection Methods and the 2 sets of parameters. Only detections and misses in the slant range interval [15m 55m] are considered.*
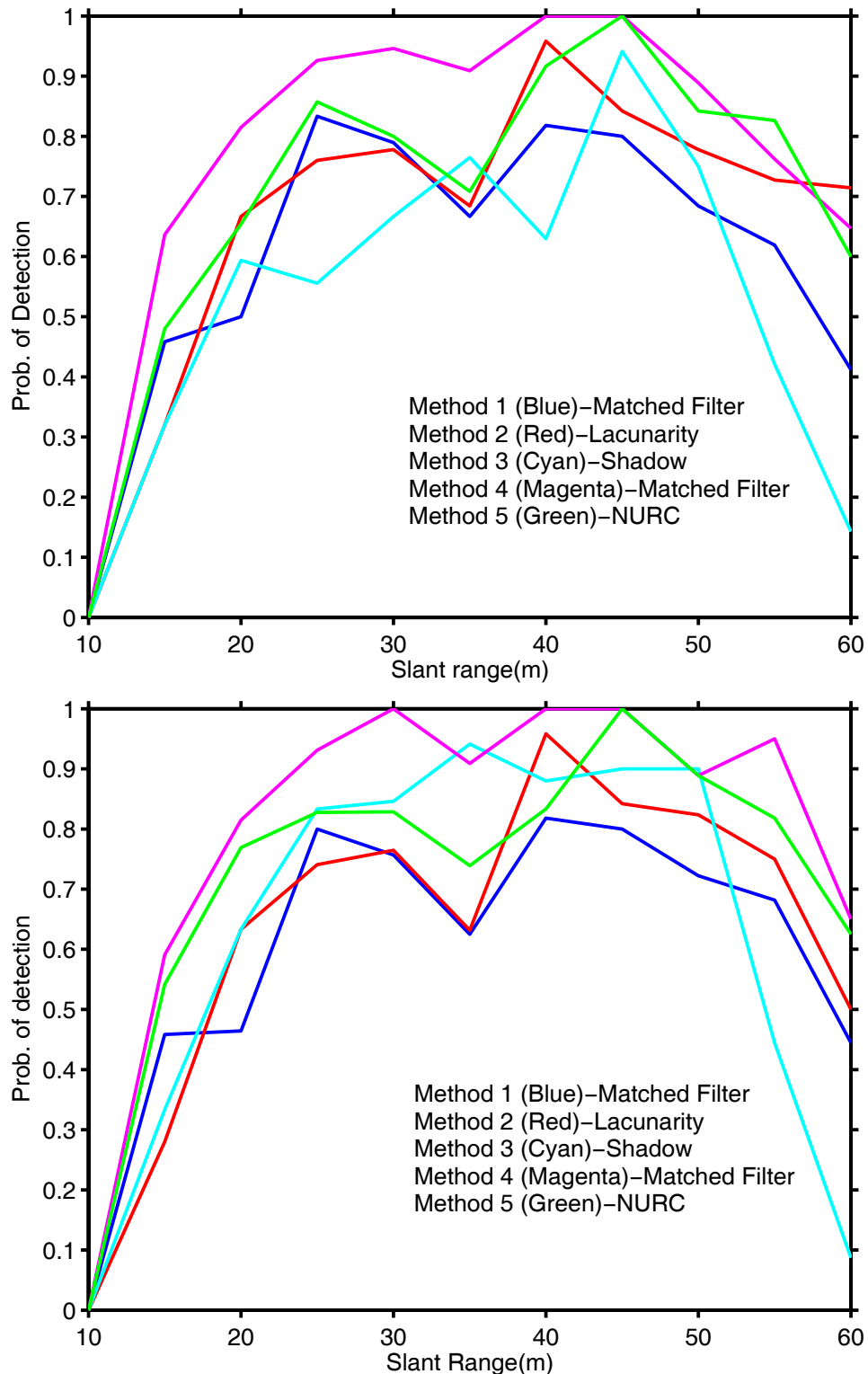
Figure 9: *Probability of detection versus slant range for the 5 methods for thresholds set to produce one false alarm/file - Site E. The top graph is for the first parameter set for each of the methods and the bottom graph is for the second set of parameters.*

4.3   Combining the outputs of the detection methods

It is often the case that the false alarms for one detection method are not the same as the false alarms for one of the other methods. This leads one to consider combining the outputs from the various detection methods to yield a better detection/false alarm rate ratio (see also, Ref.8, for the concepts of combining detector outputs) As has been discussed, we have saved the maximum values of the outputs from the various filters within the region of the sidescan image where the detection was made. These values also include the outputs from the 3 different sizes of filters used by methods 1 and 3 for the different range intervals (the hybrid filtered image is computed by using the appropriate filter output for the specified range intervals - but the values of the different size filters are, in fact, computed for the entire range interval). We can consider these values as features and train a classifier. In particular we used a kernel-based regression method as described in Ref. 1. In basic terms we seek a vector of weights a_i such that

$$\sum_{j=1}^{N} a_j exp(-|f_i - f_j|/p) = \ell_i \tag{6}$$

where f_i denotes the feature vector associated with the i'th detection, ℓ_i denotes the corresponding label ± 1 depending upon whether the detection is clutter or a target and N is the number of detections in the training set. Once the weights a_j have been determined from solving a system of equations, future detections ℓ_k are then classified as clutter or target using the relation,

$$\ell_k = 1, \quad \sum_{j=1}^{N} a_j \exp(-|f_k - f_j|/p) >= \sigma$$

$$\ell_k = -1, \quad \sum_{j=1}^{N} a_j \exp(-|f_k - f_j|/p) < \sigma \tag{7}$$

We will train using all the data of October 24 (using the first set of filter/range parameters) and test on the data from Oct.26. The feature vectors for each object are the 11 saved filter values for each of the threshold regions (we use the detection regions of Method 4). The features values are demeaned and normalized (L_1 norm) on the basis of the training set values. The parameter p in Eq.(6) is set to 3. By allowing σ to vary in Eq.(7) between, for example, ± 5 we can compute the number of correct detections and the number of false alarms which occur. In addition, we can use the determined classifier with the data of October 25 from Site E.

Another, somewhat adhoc, approach is to combine the output of Method 4 with weak constraints on the values of methods 2 and 5. In particular we will vary the threshold on Method 4 with the constraints that the output value of Method 2 should be greater

than 0.8 and the output Method 5 should be greater than 3. In the top plot of Fig. 8 we show the determined ROC curves for October 26 using just Method 4, Method 4 with the constraints and the combined classifier which was trained with the data of October 24. As can be seen, the combined classifier has the best performance. The classifier with the weak constraints on the values of the other 2 methods is slightly better than just using Method 4. In particular for the high detection rates, the number of false alarms has been decreased. In the bottom of Fig. 8 we show the results for the data of October 25. Once again including the constraints on the values of the other 2 classifiers has improved the detector performance, with a slightly smaller false alarm rate for high detection rates. The trained method (trained with data from Site D, October 24) is best in the region of probability of detection 75-85%. The improvements in the ROC curve for this method are not as significant as for the data of October 26. However, it is encouraging that this combined method, which was trained from data from one site, still gives very good performance at another site.
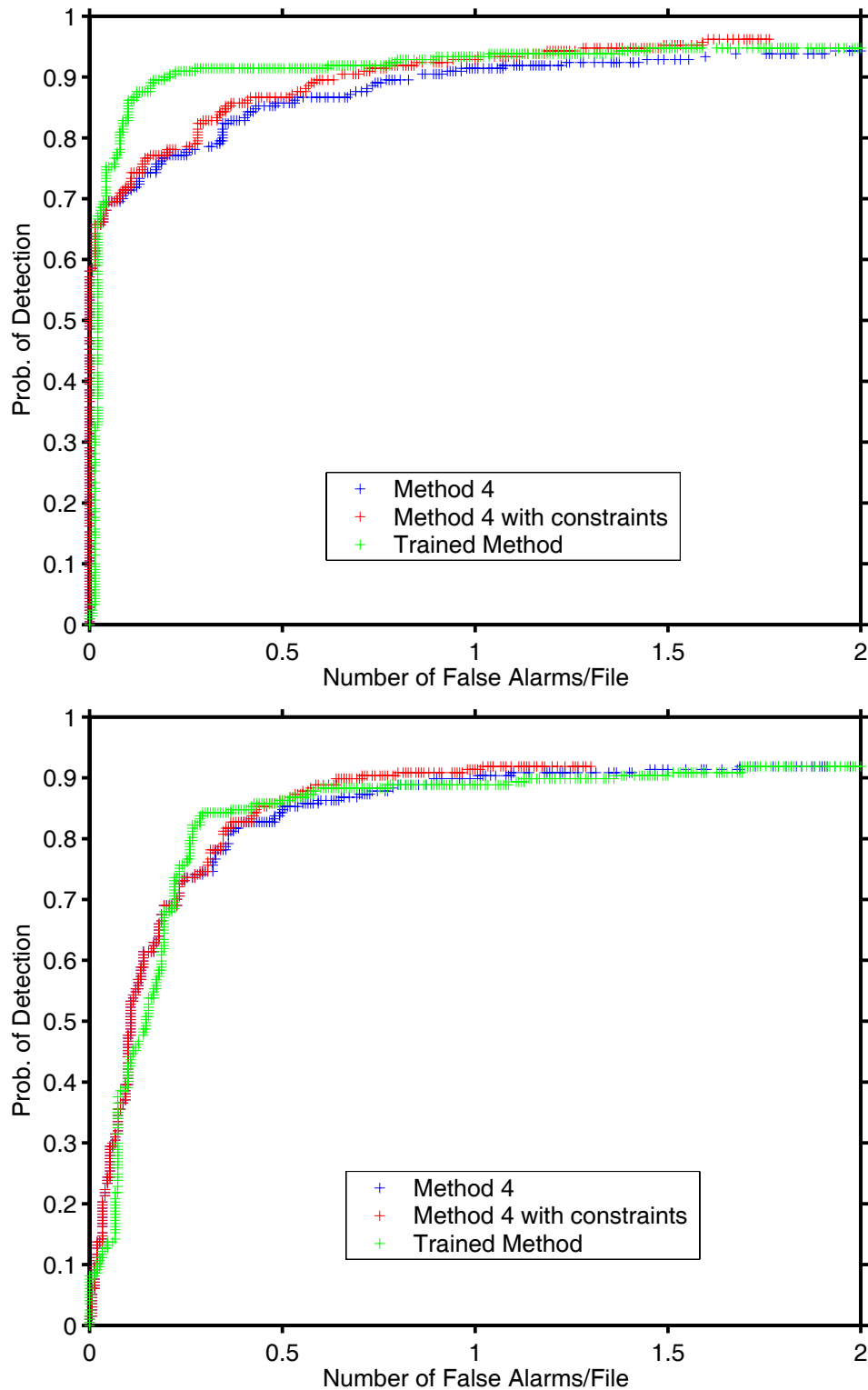
Figure 10: *The ROC curves for the site D data, Oct.26, and Site E, Oct.25 data for Method 4, Method 4 with constraints on the values corresponding to Methods 2 and 5, and a trained detector (data of October 24).*

5   SUMMARY

In this report we considered 5 different detection methods and combinations of these detection methods for the sidescan sonar data obtained during the CITADEL trials. In general, the detectors had good detection rates for all target types, although for a fixed small false alarm rate, target B seemed to be the most difficult to detect. However, Method 4 was able to detect these targets with a rate of above 90% for a false alarm rate of 2 false alarms/per file.

When the target ranges considered were restricted to between 20 and 50 m, the detection rate was very high and there did not seem to be a significant variation of detection probability with respect to these ranges. The high detection rates were associated with quite high false alarm rates for some of the detectors and this was illustrated well by the ROC curves. The trial sites had little seabed clutter. The performance of the detectors on sonar images from the much more cluttered La Spezia harbour area indicated that the detectors' thresholds might need to be adjusted for different seabed environments.

We also combined the outputs from the various filters used for the methods by first training a classifier and by using Method 4 with constraints on some of the other filter values. These combinations of filter outputs did improve the ROC curve with respect to the baseline ROC curve of Method 4. In the case of the trained method, we used the October 24 data for Site D for training and then tested the method with the Site D data from a different day (October 26). In this case, the trained method was significantly better than the other methods. We also applied the trained method to the data from another site. In this case, any improvement was less obvious. The optimal, environmentally-robust fusion of individual detection methods is a topic which warrants further investigation.

Overall, the detection capabilities of the system, which used a Klein 5500 sonar in a low-backscatter environment were very good. High detection rates with small targets were obtained with a reasonable false alarm rate.

References

[1]   J. Fawcett and V.L. Myers, "Computer-aided classification for a database of images of minelike objects", DRDC Atlantic TM 2004-272, March 2005.

[2]   R.T. Kessel and V.L. Myers, "Discriminating man-made and natural objects in sidescan imagery: human versus computer recognition performance", Proceedings of SPIE, Vol. 5807, Automatic Target Recognition XV, May 2005, pp. 141 –152.

[3]   G.J. Dobeck, J.C. Hyland and L. Smedley, "Automated detection/classification of seamines in sonar imagery" Proc. SPIE-Int. Soc. Optics, vol. 3079, pp.90-110, 1997.

[4]   R.T. Kessel, "Using sonar speckle to identify regions of interest and for mine detection", Proceedings of the SPIE, Vol. 4742, Detection and remediation techniques for mines and minelike targets , pp.440–451, August 2002.

[5]   R.T. Kessel, "Texture-based discrimination of man-made and natural objects in sidescan sonar imagery", Proceedinsg of the SPIE, Vol. 5096, Signal processing, Sensor Fusion, and Target Recognition XII, pp. 160–168, August 1003.

[6]   B. Zerr, "Algorithme statistique de detection automatique de mines marines - Automatic naval mine detection with a statistical algorithm", GESMA RG-4896, November 2004.

[7]   Petillot, Y., Reed, S. and Myers, V. Mission planning and evaluation for minehunting AUVs with sidescan sonar: Mixing real and simulated data, Report SR-447, NATO Undersea Research Centre, La Spezia, Italy, December 2005.

[8]   T. Aridgides, M. Fernandez, and G. Dobeck, "Fusion of adaptive algorithms for the classification of sea mines using high resolution side scan sonar in very shallow water", Proceedings of Oceans 2001, pp. 135–142, Vol.1, 2001.

Distribution List

Internal Distribution

John Fawcett
Underwater Force Protection Group,
9 Grove St.,
Dartmouth, Nova Scotia, B2Y 3Z7

Anna Crawford,
Underwater Force Protection Group,
9 Grove St.,
Dartmouth, Nova Scotia, B2Y 3Z7

David Hopkin,
Underwater Force Protection Group,
9 Grove St.,
Dartmouth, Nova Scotia, B2Y 3Z7

Library (5)

External Distribution

LCdr J.T. Hewitt,
DMRS 3-2, NDHQ,
101 Colonel By Dr.,
Ottawa, Ont., K1A 0K2.

NDHQ/DRDKIM

Vincent Myers,
NATO Undersea Research Centre,
Viale San Bartolomeo 400,
19138 La Spezia (SP),
Italy

Benoit Zerr,
GESMA,
BP 42, 29240 Brest Naval,
France

DOCUMENT CONTROL DATA		
(Security classification of title, body of abstract and indexing annotation must be entered when the overall document is classified)		

1. ORIGINATOR (the name and address of the organization preparing the document. Organizations for whom the document was prepared, e.g. Centre sponsoring a contractor's report, or tasking agency, are entered in section 8.) Defence R&D Canada – Atlantic, P.O. Box 1012, Dartmouth, NS, B2Y 3Z7	2. SECURITY CLASSIFICATION (overall security classification of the document including special warning terms if applicable). UNCLASSIFIED

3. TITLE (the complete document title as indicated on the title page. Its classification should be indicated by the appropriate abbreviation (S,C,R or U) in parentheses after the title). Computer-aided detection of targets from the Citadel trial Klein sonar data

4. AUTHORS (Last name, first name, middle initial. If military, show rank, e.g. Doe, Maj. John E.) Fawcett, John A.; Crawford, Anna; Hopkin, David; Myers, Vincent; Zerr, Benoit

5. DATE OF PUBLICATION (month and year of publication of document) August 2006	6a. NO. OF PAGES (total containing information Include Annexes, Appendices, etc). 35 (approx.)	6b. NO. OF REFS (total cited in document) 8

7. DESCRIPTIVE NOTES (the category of the document, e.g. technical report, technical note or memorandum. If appropriate, enter the type of report, e.g. interim, progress, summary, annual or final. Give the inclusive dates when a specific reporting period is covered). Technical Memorandum

8. SPONSORING ACTIVITY (the name of the department project office or laboratory sponsoring the research and development. Include address). Defence R&D Canada – Atlantic PO Box 1012 Dartmouth, NS, Canada B2Y 3Z7

9a. PROJECT OR GRANT NO. (if appropriate, the applicable research and development project or grant number under which the document was written. Please specify whether project or grant). 11CL	9b. CONTRACT NO. (if appropriate, the applicable number under which the document was written).

10a ORIGINATOR'S DOCUMENT NUMBER (the official document number by which the document is identified by the originating activity. This number must be unique to this document.) DRDC Atlantic TM 2006-115	10b OTHER DOCUMENT NOs. (Any other numbers which may be assigned this document either by the originator or by the sponsor.)

11. DOCUMENT AVAILABILITY (any limitations on further dissemination of the document, other than those imposed by security classification) (X) Unlimited distribution (   ) Defence departments and defence contractors; further distribution only as approved (   ) Defence departments and Canadian defence contractors; further distribution only as approved (   ) Government departments and agencies; further distribution only as approved (   ) Defence departments; further distribution only as approved (   ) Other (please specify)

12. DOCUMENT ANNOUNCEMENT (any limitation to the bibliographic announcement of this document. This will normally correspond to the Document Availability (11). However, where further distribution (beyond the audience specified in (11) is possible, a wider announcement audience may be selected).

13. ABSTRACT (a brief and factual summary of the document. It may also appear elsewhere in the body of the document itself. It is highly desirable that the abstract of classified documents be unclassified. Each paragraph of the abstract shall begin with an indication of the security classification of the information in the paragraph (unless the document itself is unclassified) represented as (S), (C), (R), or (U). It is not necessary to include here abstracts in both official languages unless the text is bilingual).

In October 2005, DRDC Atlantic participated with NURC (NATO) and GESMA (France) in a joint trial with the remote, semi-submersible vehicle DORADO. A large number of sidescan sonar images of minelike objects on the seabed were obtained for a variety of ranges and aspects. The positions of these dummy targets are very accurately known. In this particular report, we use this data to investigate the performance of 5 simple detection algorithms. Each of the 5 detectors is based upon the outputs of some simple image/filter convolutions. The detections, false alarms, and missed target statistics are presented, as well as an analysis of the missed target statistics as a function of target type and range. The performance of the detectors as their decision threshold is varied (ROC curves) is presented. In addition, the performance gains which can be achieved by combining detectors, or their corresponding filter outputs, are considered.

14. KEYWORDS, DESCRIPTORS or IDENTIFIERS (technically meaningful terms or short phrases that characterize a document and could be helpful in cataloguing the document. They should be selected so that no security classification is required. Identifiers, such as equipment model designation, trade name, military project code name, geographic location may also be included. If possible keywords should be selected from a published thesaurus. e.g. Thesaurus of Engineering and Scientific Terms (TEST) and that thesaurus-identified. If it not possible to select indexing terms which are Unclassified, the classification of each should be indicated as with the title).

detection, sonar

This page intentionally left blank.

Defence R&D Canada

Canada's leader in defence
and National Security
Science and Technology

R & D pour la défense Canada

Chef de file au Canada en matière
de science et de technologie pour
la défense et la sécurité nationale

DEFENCE **R&D** DÉFENSE

www.drdc-rddc.gc.ca